An Improved Speed Estimation Scheme for Induction Motor Drive in the Field Weakening Region

Myoung-Ho Shin, Dae-il Kim, and Dong-Seok Hyun
Department of Electrical Engineering, Hanyang University, Seongdong-ku, 133-791, Seoul, Korea

Abstract - In a conventional speed sensorless stator flux-oriented (SFO) induction machine drive system, the estimated speed is delayed in transients by the use of a low pass filter. This paper investigates the problem of a conventional speed sensorless SFO system due to the delay of the estimated speed in the field weakening region. In addition, this paper proposes a method to estimate exactly speed by using Kalman filter. The proposed method is verified by simulation and experiment with a 5-hp induction motor drive.

I. INTRODUCTION

To retain maximum torque capability in the field weakening region is important in applications such as spindle drive and railway traction. In the field weakening region, the dynamic performance of the machine is affected by the current rating and the maximum voltage that the inverter can apply to the machine. Many efforts have been made to obtain maximum torque capability in the field weakening region [1]-[4].

In the speed sensorless stator flux-oriented (SFO) control system, when the estimated speed is transformed into the sampled-data model using the first-forward difference approximation, the sampled data model has a modeling error which, in turn, produces an error in the rotor speed estimation. The error included in the estimated speed is removed by the use of a low pass filter (LPF) [5]. As a result of that, the delay of the estimated speed occurs in transients by the use of the LPF.

In the field weakening region, flux reference should be reduced as speed increases. The method for the field weakening operation is to vary the stator flux reference in proportion to the inverse of the rotor speed ($1/\omega_r$ method). In this case, the base speed for field weakening operation is determined considering maximum torque capability. In the system with a speed sensor, the appropriate base speed is determined considering the maximum torque capability. However, in the speed sensorless system, the appropriate base speed could not be determined because of the delay of the estimated speed in transients. Consequently, by the delay of the onset of field weakening region due to the delay of the estimated speed, the inverter runs out of voltage, and current regulation is lost.

This paper investigates the problem of the conventional field weakening method of a speed sensorless SFO system and proposes a new speed estimation scheme to estimate speed exactly in transients in the field weakening region. The error included in the estimated speed is removed by not a low pass filter but Kalman filter so that exact speed estimation in transients is achieved. The effectiveness of the proposed scheme is verified by comparing the proposed scheme with a conventional scheme.

II. CONVENTIONAL METHOD

In the conventional SFO system, the field weakening method is to vary the stator flux reference in proportion to the inverse of the rotor speed.

$$\lambda_{ds}^{*} = \frac{\omega_b}{\omega_r}\lambda_{ds\_rated}^{*} \qquad (1)$$

where '*' = reference value, λ_{ds} =d-axis stator flux, $\lambda_{ds\_rated}^{*}$ = rated d-axis stator flux reference, ω_b = base speed, and ω_r = rotor angular speed. In speed sensorless SFO system, the estimated rotor speed should be used to obtain the stator flux reference because the speed sensor is not used.

In SFO system, estimated synchronous angular frequency in stationary $\alpha-\beta$ reference frame can be given as [1]

$$\hat{\omega}_e = \frac{(v_{\beta s} - R_s i_{\beta s})\hat{\lambda}_{\alpha s} - (v_{\alpha s} - R_s i_{\alpha s})\hat{\lambda}_{\beta s}}{\left|\hat{\lambda}_s\right|^2} \qquad (2)$$

where '^' = estimated value; R_s = stator resistance; $v_{\alpha s}$, $v_{\beta s}$ = α and β-axis components of stator voltage; $i_{\alpha s}$, $i_{\beta s}$ = α and β-axis components of stator current; $\lambda_{\alpha s}$, $\lambda_{\beta s}$ = α and β-axis components of stator flux.

The estimated slip angular frequency in rotating d-q reference frame, the estimated mechanical rotor speed, and the estimated rotor position can be given as, respectively, [1]

$$\hat{\omega}_{sl} = \frac{(1+\sigma\tau_r p)L_s i_{qs}}{\tau_r(\hat{\lambda}_{ds} - \sigma L_s i_{ds})} \qquad (3)$$

$$\hat{\omega}_r = \frac{2}{P}(\hat{\omega}_e - \hat{\omega}_{sl}) \qquad (4)$$

$$\hat{\theta}_r = \int \hat{\omega}_r dt \qquad (5)$$

where L_s = stator self inductance, σ= total leakage factor $(=1-L_m^2/L_sL_r)$, L_m = magnetizing inductance, L_r = rotor self inductance, p= differential operator, τ_r = rotor time constant $(=L_r/R_r)$, R_r = rotor resistance, P = number of poles.

Equation (2) is transformed into the sampled-data model using the first-forward difference approximation. It is noted that the sampled data model of (2) has a modeling error which, in turn, produces an error in rotor speed estimation. This error is removed by the use of a low pass filter [5]. However, the estimated rotor speed is delayed by the use of the LPF in transients. The onset of the field weakening region is also delayed due to the delay of the estimated rotor speed. Consequently, the flux level is too high due to the delay of the onset in transient so that the inverter runs out of voltage and current regulation is lost.

III. SPEED ESTIMATION BY KALMAN FILTER

Dynamic equation can be given as

$$J_m \frac{d\omega}{dt} + B_m \omega = u + \tau_d \tag{6}$$

where ω = mechanical angular velocity, J_m = inertia moment, B_m = viscous coefficient, u = driving torque, τ_d = disturbance load torque.

Mechanical angular rotor speed is given as

$$\omega = \frac{d\theta}{dt} \tag{7}$$

where θ = mechanical angular position.

It is assumed that disturbance load torque τ_d is constant for one sampling period because the load torque is very slowly changed for sampling period.

$$\frac{d\tau_d}{dt} = 0 \tag{8}$$

State equations can be given as (9) and (10) from (6), (7), and (8).

$$\frac{dx}{dt} = Ax + Bu \tag{9}$$

$$y = Cx \tag{10}$$

where $A = \begin{bmatrix} -B_m / J_m & 0 & 1/J_m \\ 1 & 0 & 0 \\ 0 & 0 & 0 \end{bmatrix}$, $B = [1/J_m \quad 0 \quad 0]^T$,

$C = [0 \quad 1 \quad 0]$, $x = [\hat{\omega} \quad \hat{\theta} \quad \hat{\tau}_d]^T$.

In the real system, some uncertainties in the model and environment as modeling inaccuracies, disturbances and noises should be considered. State equations with random noises can be given as (11) and (12).

$$\frac{dx}{dt} = Ax + Bu + \Gamma\xi \tag{11}$$

$$y = Cx + \eta \tag{12}$$

where ξ and η are zero-mean white gaussian noise inputs, with covariance matrix Q and R, respectively. Γ, ξ, and η are given as

$$\Gamma = \begin{bmatrix} 1/J_m & 0 \\ 0 & 0 \\ 0 & 1 \end{bmatrix}, \ \xi = [u_{noise} \quad \tau_{noise}]^T, \ \eta = \theta_{noise}$$

where u_{noise} = system noise included in control input, τ_{noise} = system noise included in disturbance load torque, θ_{noise} = noise produced by transforming rotor position of (5) into the sampled-data model.

The matrix Q means the disturbances such as the error produced by transforming into sampled data system, the error by the imperfection of current controller, and modeling error of torque constant, viscous friction and the moment of inertia. The matrix R describes the noise produced by transforming the estimated rotor position (5) into sampled data model. Q and R can be given as

$$Q = \begin{bmatrix} q_{00} & 0 \\ 0 & q_{11} \end{bmatrix}, \ R = [r_{00}]$$

where q_{00} = torque reference covariance value, q_{11} = disturbance load torque covariance value, and r_{00} = covariance value of the sampled data model of the estimated rotor position (5). In the matrix Q, the off-diagonal term is zero because cross-correlation between the noise elements is very small.

Equation (11), (12) can be discretized as

$$x_{k+1} = A_k x_k + B_k u_k + \Gamma_k \xi_k \tag{13}$$

$$y_k = C_k x_k + \eta_k \tag{14}$$

where $A_k = e^{AT}$, $B_k = \int_0^T e^{A\tau} B d\tau$, $\Gamma_k = \int_0^T e^{A\tau} \Gamma d\tau$, $C_k = [0 \quad 1 \quad 0]$, and A_k, B_k, and Γ_k are approximated with $e^x \approx 1 + x$.

The Kalman filter algorithm is given by [6]

$$P_0 = Var(x_0) \tag{15}$$

$$\hat{x}_0 = E(x_0) \tag{16}$$

$$P_k^- = A_k P_{k-1} A_k^T + \Gamma_k Q \Gamma_k^T \tag{17}$$

$$\hat{x}_k^- = A_k \hat{x}_{k-1} + B_k u_{k-1} \tag{18}$$

$$K_k = P_k^- C_k^T (C_k P_k^- C_k^T + R)^{-1} \tag{19}$$

$$P_k = (I - K_k C_k) P_k^- \tag{20}$$

$$\hat{x}_k = \hat{x}_k^- + K_k (y_k - C_k \hat{x}_k^-) \tag{21}$$

where $Var(x)$ = the variance of x, $E(x)$ = the expectation of x, K_k = the Kalman gain matrix, P_k = error covariance matrix, y_k = the estimated rotor position of (5).

Kalman filter algorithm is suitable to the system which has many unknown noises such as current ripple by PWM, noise by modeling error, measurement error, and so forth. Those noises are treated as a disturbance torque in Kalman filter algorithm. The noise produced by transforming the estimated rotor position (5) into sampled data model is removed by treating the noise as a disturbance torque in Kalman filter. Fig. 1 shows the block diagram of speed controller and disturbance torque observer that incorporates Kalman filter. The inertia moment is estimated by the method in [7].

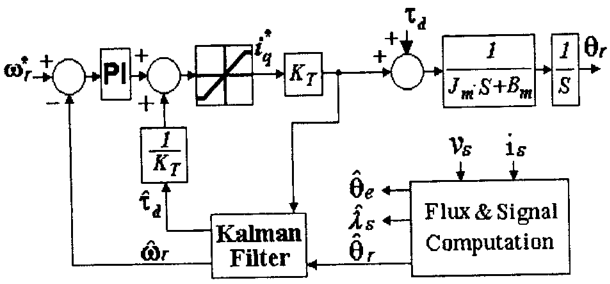

Fig. 1. Block diagram of speed controller and disturbance torque observer that incorporates Kalman filter.

IV. A DIRECT STATOR FLUX-ORIENTED SYSTEM

The control scheme of the proposed drive system is stator flux orientation. Fig. 3 shows the control block diagram of stator flux-oriented control drive that incorporates the proposed scheme. The stator flux magnitude and the transformation angle can be written as follows from the stator flux in stationary α-β reference frame.

$$|\hat{\lambda}_s| = \hat{\lambda}_{ds} = \sqrt{\hat{\lambda}_{\alpha s}^2 + \hat{\lambda}_{\beta s}^2} \tag{43}$$

$$\cos(\hat{\theta}_e) = \frac{\hat{\lambda}_{\alpha s}}{|\hat{\lambda}_s|}, \quad \sin(\hat{\theta}_e) = \frac{\hat{\lambda}_{\beta s}}{|\hat{\lambda}_s|} \tag{44}$$

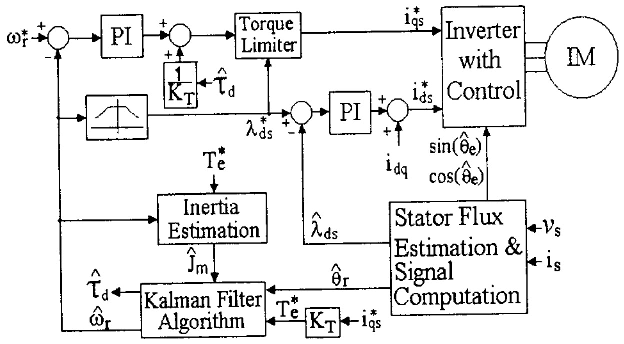

Fig. 3. Block diagram of stator flux-oriented control drive that incorporates the proposed scheme.

The decoupling compensator is represented in rotating d-q reference frame as (45) [8].

$$i_{dq} = \frac{\hat{\omega}_{sl}\tau_r \sigma i_{qs}}{(1+\sigma\tau_r p)} = \frac{i_{qs}^2 \sigma L_s}{\hat{\lambda}_{ds} - \sigma L_s i_{ds}} \tag{45}$$

The stator voltage is reconstructed from the inverter switching states [9]. A switching function SA for phase A is 1 when upper switch of phase A is on. SA is 0 when lower switch of phase A is on. A similar definition is adopted for phase B and C. The stator voltage in stationary α-β reference frame can be given as

$$v_{\alpha s} = \frac{V_{dc}}{3}(2SA - SB - SC) \tag{46}$$

$$v_{\beta s} = \frac{V_{dc}}{\sqrt{3}}(SB - SC) \tag{47}$$

The processor reads the outputs of prefilter(s= -2985) through an A/D converter.

The stator flux can be estimated by the integration of back emf. The stator fluxestimation by pure integrator has drift and saturation problems. To solve the problems, in this paper, the following programmable low pass filter is used [10].

$$\hat{\lambda}_s = \frac{(v_s - R_s i_s)}{s + |\hat{\omega}_e|/3} \frac{\sqrt{\hat{\omega}_e^2 + (\hat{\omega}_e/3)^2}}{|\hat{\omega}_e|} \exp(-j\phi_1) \times \frac{\sqrt{\hat{\omega}_e^2 + 2985^2}}{2985} \exp(j\phi_2) \tag{48}$$

where $\phi_2 = \tan^{-1}(\hat{\omega}_e / 2985)$,

$$\cos(\phi_1) = \frac{|\hat{\omega}_e|}{\sqrt{\hat{\omega}_e^2 + (\hat{\omega}_e/3)^2}}, \sin(\phi_1) = \frac{\hat{\omega}_e/3}{\sqrt{\hat{\omega}_e^2 + (\hat{\omega}_e/3)^2}}.$$

The pole ($|\hat{\omega}_e|/3$) of programmable LPF is increased to decrease the time constant of the programmable LPF as speed increases. The constant "3" in $|\hat{\omega}_e|/3$ was selected by trial and error for good performance.

V. SIMULATION RESULTS

The proposed scheme was studied by simulation with the drive system shown in Fig. 3. The motor parameters are shown in Table I.

TABLE I INDUCTION MOTOR PARAMETERS

5 hp, 220 V, 4 poles, 60 Hz		
Rated flux	0.42	(Wb)
Rated line current(peak)	18.2	(A)
Stator resistance	1.26	(Ω)
Rotor resistance	0.2	(Ω)
Magnetizing inductance	50	(mH)
Stator leakage inductance	4.7	(mH)
Rotor leakage inductance	4.7	(mH)
Inertia moment	0.01	(kg·m)

Fig. 4 shows the estimated speeds by Kalman filter and LPF when speed reference is changed from 1000 (rpm) to 4000 (rpm). The measured speed ω_r is controlled and used for field weakening operation. The base speed is 1805 (rpm). With this base speed, it is seen that the current is well regulated in the field weakening region. If a base speed higher than 1805 (rpm) is selected, the inverter runs out of voltage, and current regulation is lost. In the conventional method, the cutoff frequency of the LPF is 6.366Hz. It can be seen that the estimated speed $\hat{\omega}_{r,LPF}$ by the LPF is delayed in transient due to the use of the LPF. However, the estimated speed $\hat{\omega}_{r,KF}$ by Kalman filter is not delayed in transient. In the conventional method, if the cutoff frequency of the LPF is increased, the delay of the estimated speed in transient is decreased. However, the speed estimation become unstable.

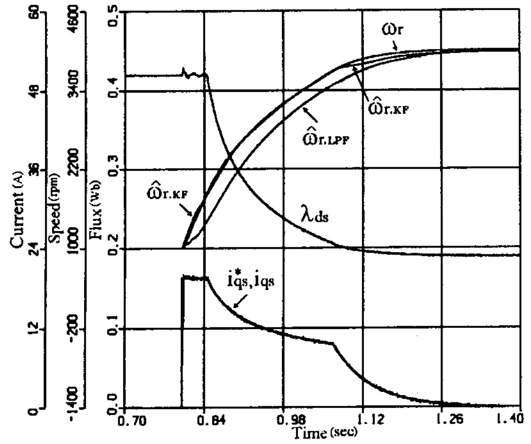

Fig. 4. Estimated speeds by LPF and estimated speed by Kalman filter when the real speed is controlled and used for field weakening operation.

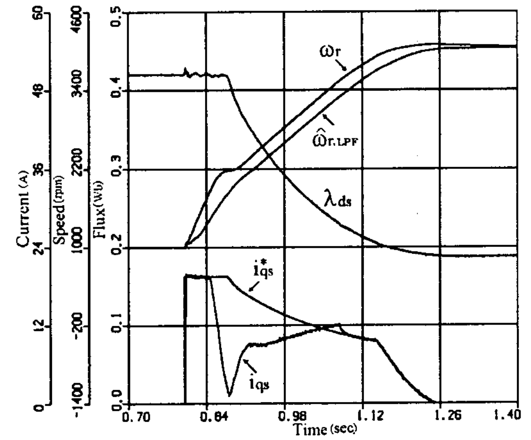

Fig. 5. Speed and current waveforms when $\hat{\omega}_{r,LPF}$ is controlled and used for field weakening operation.

Fig. 5 shows he speed and current when $\hat{\omega}_{r,LPF}$ is controlled and the onset of field weakening region is determined according to the estimated speed $\hat{\omega}_{r,LPF}$. At the onset of field weakening region, the real speed is higher than 1805 (rpm) due to the delay of the estimated speed. As the result, the inverter runs out of voltage, and current regulation is lost. Therefore the torque is reduced and more acceleration time is needed in transient.

Fig. 6 shows the speed and the current when $\hat{\omega}_{r,KF}$ is controlled and used for field weakening operation. Because the estimated speed $\hat{\omega}_{r,KF}$ is not delayed in transient, the onset of field weakening region is not delayed. As the result, it is seen that the current is well regulated.

VI. EXPERIMENTAL RESULTS

In order to verify the proposed scheme, the control system was implemented by the software of DSP TMS320C31. The inverter input voltage is V_{dc}=325 (V). The switching frequency is 4 (kHz). The current control period is 125 (μs). The speed control period is 1.25 (ms). The stator currents are detected through Hall-type sensors. The stator currents are sampled and held at every sampling instant, then A/D converted with 3.5 (μs) conversion time. Kalman filter algorithm is divided into two parts. Each is executed every 125 (μs) and the estimated states are employed every 250 (μs). q_{00}, q_{11}, r_{00}, and λ are set to 1.0, 0.01, 0.01, and 30. The motor is 5 (hp) three-phase induction motor shown in Table I.

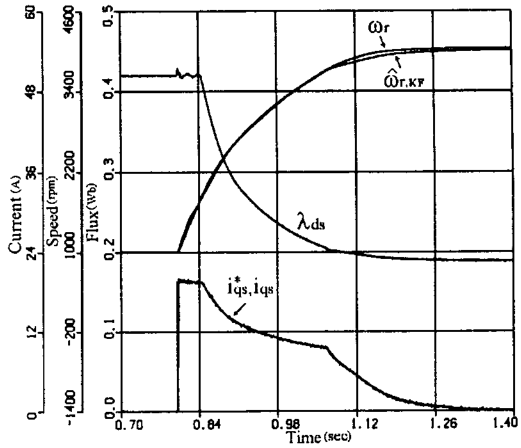

Fig. 6. Speed and current waveforms when $\hat{\omega}_{r,KF}$ is controlled and used for field weakening operation.

Fig. 7 shows the speed, current, and flux when the measured speed is controlled and used for field weakening operation. The base speed is 1805 (rpm). If a base speed higher than 1805 (rpm) is selected, the inverter runs out of voltage, and current regulation is lost. Fig. 7(a) shows the estimated speed $\hat{\omega}_{r,LPF}$ is delayed in transient due to the use of LPF. Fig. 7(b) shows the estimated speed $\hat{\omega}_{r,KF}$ is not delayed in transient. Fig. 7(c) shows that the q-axis current is well regulated.

Fig. 8(a) shows measured speed $\omega_{r,LPF}$ and $\omega_{r,KF}$ when $\hat{\omega}_{r,LPF}$ and $\hat{\omega}_{r,KF}$ are controlled, respectively. Fig. 8(b) shows the current when $\hat{\omega}_{r,KF}$ is controlled. Fig. 8(c) shows the current when $\hat{\omega}_{r,LPF}$ is controlled. In Fig. 8(c), it is seen that current regulation is lost since the onset of field weakening region occurs in the speed more than 1805(rpm) due to the delay of the estimated speed $\hat{\omega}_{r,LPF}$. As the result of that, in Fig. 8(a), it is seen that the measured speed $\omega_{r,LPF}$ requires more acceleration time than $\omega_{r,KF}$. In Fig. 8(d), it is observed that the estimated flux $\hat{\lambda}_{ds,LPF}$ is higher than $\hat{\lambda}_{ds,KF}$ since the onset of field weakening region of the conventional method is delayed.

VII. CONCLUSION

This paper investigated the problem of conventional field weakening method of speed sensorless SFO system and proposed a new speed estimation scheme to estimate speed exactly in transients in the field weakening region. The error included in the estimated rotor speed was removed by not a low pass filter but Kalman filter.

In the conventional method the performance in the field weakening region was deteriorated due to the delay of estimated speed. However, in the proposed method, the estimated speed was not delayed and the performance was not deteriorated in the field weakening region.

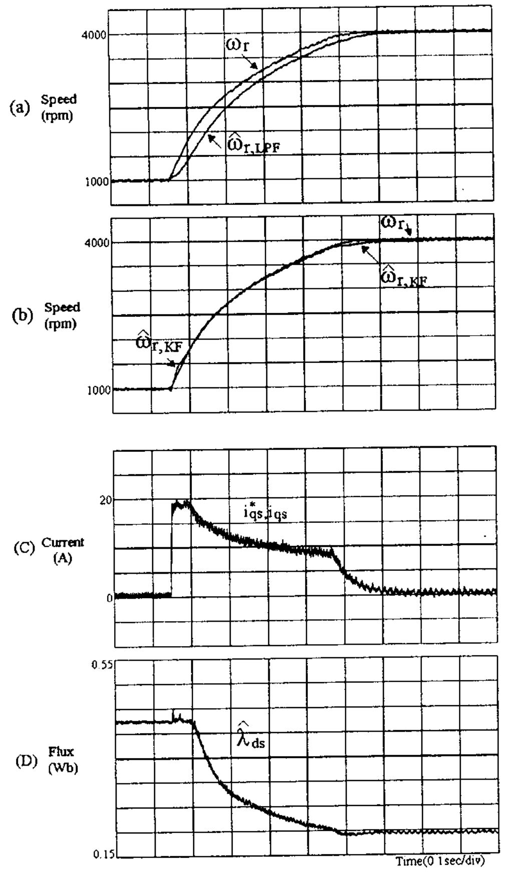

Fig. 7. Estimated speed $\hat{\omega}_{r,LPF}$, $\hat{\omega}_{r,KF}$, current, and flux when the measured speed is controlled and used for field weakening operation.

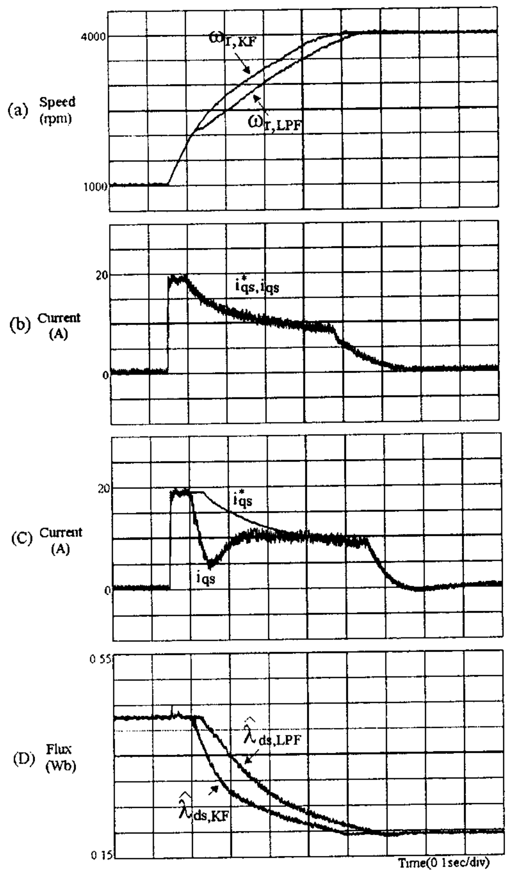

Fig. 8. Speed, current and flux (a) measured speed when $\hat{\omega}_{r,LPF}$ and $\hat{\omega}_{r,KF}$ are controlled, respectively (b) current when $\hat{\omega}_{r,KF}$ is controlled (c) current when $\hat{\omega}_{r,LPF}$ is controlled (d) estimated flux when $\hat{\omega}_{r,LPF}$ and $\hat{\omega}_{r,KF}$ are controlled, respectively.

REFERENCES

[1] X. Xu and D. W. Novotny, "Selection of the Flux Reference for Induction Machine Drives in the Field Weakening Region," *IEEE Trans. Indus. Appli.*, vol. 28, no.6, pp.1353-1358, 1992.

[2] Y. T. Kao and C. H. Liu, "Analysis and Design of Microprocessor-Based Vector-Controlled Induction Motor Drives," *IEEE Trans. Ind. Electron.*, vol. 39, no. 1, pp.46-54, 1992.

[3] S. H. Kim and S. K. Sul, "Maximum Torque Control of an Induction Machine in the Field Weakening Region," *IEEE Trans. Indus. Appli.*, vol 31, no.4, pp. 787-794, 1995.

[4] M. H. Shin, D. S. Hyun, and S. B. Cho, "Maximum Torque Control of Stator Flux-Oriented Induction Machine Drive in the Field Weakening Region," in *Proc. IEEE IAS Ann. Meet.*, pp. 1461-1467, Oct. 2000.

[5] L. Ben-Brahim, and A. Kawamura, "A Fully Digitized Field-Oriented Controlled Induction Motor Drive Using Only Current Sensors," *IEEE Trans. Ind. Electron.*, vol. 39, no. 3, pp.241-249, 1992.

[6] M. S. Grewal and A. P. Andrews, *Kalman Filter Theory and Practice*, Prentice Hall, 1993.

[7] I. Awaya, Y. Kato, I. Miyake and M. Ito, "New Motion Control with Inertia Identification Function Using Disturbance Observer," in *Proc. IECON'92* pp.77-81, 1992.

[8] X. Xu, R D. Doncker and D. W. Novotny, "A Stator Flux Oriented Induction Machine Drive," *IEEE Power Electron. Specialists Conf.* pp. 870-876, 1988.

[9] T. G. Habetler and D. M. Divan, "Control Strategies for Direct Torque Control Using Discrete Pulse Modulation," in *Proc. IEEE IAS Ann. Meet.*, pp. 514-522, Oct. 1989.

[10] M. H. Shin, D. S. Hyun, S. B. Cho, and S. Y. Choe, "An Improved Stator Flux Estimation for Speed Sensorless Stator Flux Orientation Control of Induction Motors," *IEEE Trans. PE*, vol. 15, no. 2, pp. 312-318, 2000.